

# Energy Transmission across Acoustically Mismatched Solid Junctions

Jian Wang and Jian-Sheng Wang

*Department of Computational Science, National University of Singapore, Singapore 117543, Republic of Singapore*

(Dated: 3 September 2005)

We derive expression for energy flux in terms of lattice normal mode coordinates. Energy transmission across solid junctions from lattice dynamic point of view is given and its relation with atomic masses, lattice constants, and group velocities is clarified. A scattering boundary method (SBM) is proposed for calculating the amplitude transmission across solid junctions. The phonon transmission coefficients and thermal conductance are calculated for two kinds of acoustically mismatched junctions: different chirality nanotubes (11, 0) to (8, 0), and Si-Ge interface structure. Our calculation shows a mode-dependent transmission in nanotube junction due to the high symmetry vibrating motions for nanotube atoms, indicating its possible important role in nanotube mixture thermal conductance. Energy transmission and Kapitza conductance across the Si-Ge interface [001] are calculated for the Si-Ge diamond-type structure. It is shown that the energy transmission across the Si-Ge interface depends on the incident angle and on the interface mode conversion. A critical incident angle about  $42^\circ$  is numerically found for waves incident from Ge to Si. Our numerical result of the Kapitza conductance at temperature  $T = 200$  K is  $G_K = 4.6 \times 10^8$  WK $^{-1}$ m $^{-2}$ . We find numerically scaling law  $G_K \propto T^{2.87}$  for [001] interface at low temperature.

PACS numbers: 66.70.+f, 44.10.+i, 05.45.-a

## I. INTRODUCTION

Rapid progress in the synthesis and processing of materials with structures of nanometer length scales has created a demand for the understanding of thermal transport in nano-scale low dimensional devices<sup>1,2,3,4</sup>. Recent experimental and theoretical studies have revealed novel features of phonon transport in these systems, such as the size-dependent anomalous heat conduction in one-dimensional (1D) chain<sup>2</sup> and the universal quantum thermal conductance<sup>3</sup>. Thermal transport in nanostructures may differ from the predictions of Fourier's law based on bulk materials; this may happen because of the existence of many acoustically mismatched interfaces in nanostructures and because the phonon mean free path is comparable to the size of the structure<sup>4</sup>. An understanding of the thermal conduction across acoustically mismatched solid interfaces is a necessary requirement for thermal transport engineering.

The study of thermal transport across interfaces dates back as early as to 1940s when Kapitza resistance<sup>5</sup> was reported and much work has been done in this field<sup>4,5</sup>. In general, theoretical modeling of this problem has been undertaken either by the acoustic-mismatch model (AM) with scalar elastic waves, or by the diffuse-mismatch model (DM) with Boltzmann transport equation<sup>6</sup>. Some numerical methods such as molecular dynamic simulation<sup>7</sup> have also been used. While AM and DM models provide some useful reference calculations, scalar wave model and Boltzmann transport equation are only phenomenological descriptions and they have ignored the complexity of the interface. Atomic-level lattice dynamic (LD) approach should be the right way of capturing the mechanism of heat transport. Authors in Ref. 8 have proposed to calculate the amplitude transmission by connecting the neighboring atoms

through the dynamic equations across the interface. Ref. 9 has suggested calculating the phonon transport via Green's functions. However, the Green's function method gives only a formal solution for the scattering problem. A practical calculation procedure is not provided. Ref. 8 used phonon mode of wave incident from one lead to calculate the energy transmission through the amplitudes of the transmitted/reflected waves by  $t_{\mathbf{k}j} = \rho_A \sum_q v_{qz} A_q^2 / (\rho_B v_{0z} A_0^2)$  without any justification. How to calculate the energy transmission from the amplitudes of the transmitted/reflected waves, and what is its relationship with atom mass, lattice constant and group velocity? It's not clear. On the other hand, the well-known Landauer formula for electronic conduction<sup>10</sup> can be generalized to thermal transport for such calculations. Landauer formula for ballistic heat transport across junctions has been used<sup>11,12</sup> for the prediction of universal quantum heat conductance at very low temperatures. The energy transmission formula derived under continuum assumption may not be applied straightforwardly to systems on nanoscale where atomic details are important.

In this paper, we report our results of the energy transmission across solid junctions taking into account atomic details from lattice dynamic point of view both theoretical and numerically. In Section II, we will first derive the energy flux by lattice dynamics method and then give the energy transmission across the interface involving atomic mass, lattice constant and group velocity, starting from the energy conservation law. An analytic result for 1D acoustic mismatched chain model from our formula is also illustrated. We further propose computing the amplitude transmission coefficients by solving a set of dynamical equations with a scattering boundary condition method (SBM) to cope with the complex interface. In Section III, we first compute the transmission coefficient

cients of a Carbon-nanotube junction showing a mode-dependent transmission in nanotube junction due to the high symmetry of vibration in nanotubes. Then for the Si and Ge diamond-typed structure by linearized empirical Tersoff potential, we calculate the energy transmission across the Si-Ge interface [001] to show its dependence on the incident angle. A critical incident angle about  $42^\circ$  is numerically found for waves incident from Ge to Si. We also calculate the Kapitza conductance for Si-Ge interface at different temperatures and find its value  $G_K = 4.6 \times 10^8 \text{ WK}^{-1} \text{ m}^{-2}$  when  $T = 200 \text{ K}$  and numerically get its scaling law  $T^{2.87}$  at low temperature.

## II. THEORY

### A. Energy Flux

In this section we derive the energy flux in terms of the normal mode coordinates of the atomic vibration from the energy continuity equation. We consider systems with perfect leads on the left and right with an arbitrary interaction at the junction. The Hamiltonian for each lead system (as well as the whole system) of vibrating atoms under linear approximation takes the form

$$H = \sum_l \left( \sum_{i,\alpha} \frac{p_{l,i}^{\alpha 2}}{2m_i} + \sum_{l',i,\alpha;j,\beta} \frac{1}{2} K_{l,i;l',j}^{\alpha,\beta} u_{l,i}^\alpha u_{l',j}^\beta \right) = \sum_l \varepsilon_l, \quad (1)$$

where  $l$  or  $l'$  denotes a unit cell,  $i, j$  the position in a cell,  $\alpha, \beta$  the direction of vibrating motions of atoms, and  $u_{l,i}^\alpha$  the displacement from equilibrium of the atom ( $l, i$ ) with equilibrium position  $\mathbf{R}_{l,i}$ . The dynamic matrix eigenvalue problem can be written as

$$\mathbf{D}\tilde{\mathbf{e}} = \omega^2 \tilde{\mathbf{e}}, \quad \|\mathbf{D} - \omega^2 \mathbf{I}\| = 0, \quad (2)$$

where  $\mathbf{D}_{i,j}^{\alpha,\beta} = \frac{1}{\sqrt{m_i m_j}} \sum_{l'} K_{l,i;l',j}^{\alpha,\beta} e^{i\mathbf{q}\cdot(\mathbf{R}_{l'} - \mathbf{R}_i)}$ . The eigenvector for Eq. (2) is  $\tilde{e}_{i,n}^\alpha(\mathbf{q})$ , where  $i$  denotes the position in a cell,  $\alpha$  the direction of vibrating motion,  $n$  the branch of polarization. These eigenvectors satisfy  $\sum_{i,\alpha} \tilde{e}_{i,n}^\alpha(\mathbf{q}) \tilde{e}_{i,n'}^{*\alpha}(\mathbf{q}) = \delta_{n,n'}$ . So the vibrating motions of atoms can be expanded into the summation of these eigenvectors

$$u_{l,i}^\alpha = \frac{1}{\sqrt{Nm_i}} \sum_{\mathbf{q},n} Q_{\mathbf{q}}^n(t) \tilde{e}_{i,n}^\alpha(\mathbf{q}) e^{i\mathbf{q}\cdot\mathbf{R}_l}, \quad (3)$$

where  $Q_{\mathbf{q}}^n(t)$  is a normal mode coordinate of the vibration, and  $N$  is the number of the unit cells. Each normal mode represents a single harmonic oscillation  $\ddot{Q}_{\mathbf{q}}^n(t) + \omega_n^2(\mathbf{q}) Q_{\mathbf{q}}^n(t) = 0$ . A local energy density can be defined through the energy in cell  $l$  from Eq. (1), as  $\rho(\mathbf{r}) = \sum_l \varepsilon_l \delta(\mathbf{r} - \mathbf{R}_l)$  where  $\mathbf{R}_l$  is a lattice vector.

Next, an expression for the energy current in the  $z$  direction can be derived from the energy continuity equation,  $\partial\rho/\partial t + \nabla \cdot \mathbf{j} = 0$ , where  $\mathbf{j}$  is the energy current

density. We transform the energy continuity equation into the momentum space,

$$\left\langle \dot{\Omega}(\mathbf{q}, t) \right\rangle_t + iq_z \langle J_z(\mathbf{q}, t) \rangle_t = 0, \quad (4)$$

by the following Fourier transform

$$\rho(\mathbf{r}, t) = \frac{1}{(2\pi)^3} \int \Omega(\mathbf{q}, t) e^{i\mathbf{q}\cdot\mathbf{r}} d^3\mathbf{q}, \quad (5)$$

$$\mathbf{j}(\mathbf{r}, t) = \frac{1}{(2\pi)^3} \int \mathbf{J}(\mathbf{q}, t) e^{i\mathbf{q}\cdot\mathbf{r}} d^3\mathbf{q}. \quad (6)$$

In these equations,  $\Omega(\mathbf{q}, t)$  and  $\mathbf{J}(\mathbf{q}, t)$  are the energy density and energy current density in momentum space, respectively, and the bracket  $\langle \rangle_t$  denotes the time average. Here we have assumed that the energy current propagates along  $z$  direction and so the time averaged energy current components along other two directions equal to zero. A relation of the total energy current in real space and in momentum space is

$$\lim_{\mathbf{q} \rightarrow 0} \mathbf{J}(\mathbf{q}, t) = \int \mathbf{j}(\mathbf{r}, t) d^3\mathbf{r}. \quad (7)$$

Using Eq. (4) and Eq. (7), we can get the average energy flux along the  $z$  direction,

$$\bar{I}_z = \frac{\langle J_z(\mathbf{q}, t) \rangle_t}{V} = \frac{1}{V} \lim_{q_z \rightarrow 0} \frac{\langle \dot{\Omega}(\mathbf{q}, t) \rangle_t}{-iq_z}, \quad (8)$$

where  $V$  is the volume of the lead part.

With the help of Eq. (1), Eq. (3), and Eq. (5), the energy density in momentum space is given by

$$\Omega(\mathbf{q}_0, t) = \sum_l \varepsilon_l e^{-i\mathbf{q}_0 \cdot \mathbf{R}_l} = \frac{1}{2} \sum_{\mathbf{q}, \mathbf{q}', n, n'} \left\{ (\dot{Q}_{\mathbf{q}}^n \dot{Q}_{\mathbf{q}'}^{n'}) + \omega_{n'}^2(\mathbf{q}') Q_{\mathbf{q}}^n Q_{\mathbf{q}'}^{n'} \right\} \times \sum_{i,\alpha} \tilde{e}_{i,n}^\alpha(\mathbf{q}) \tilde{e}_{i,n'}^{*\alpha}(\mathbf{q}') \delta_{\mathbf{q}+\mathbf{q}', \mathbf{q}_0}, \quad (9)$$

where  $Q_{\mathbf{q}}^n$ 's are normal mode coordinates for the  $n$ -th branch phonons. Combining Eq. (8) and Eq. (9), the time-averaged energy flux along  $z$ -direction is

$$\bar{I}_z = \frac{-i}{V} \sum_{\mathbf{q}, n} \omega_n(\mathbf{q}) \frac{\partial \omega_n(\mathbf{q})}{\partial q_z} \langle Q_{\mathbf{q}}^n \dot{Q}_{\mathbf{q}}^{n*} \rangle_t. \quad (10)$$

Note that during the derivation of Eq. (10),  $\Omega(\mathbf{q}, t)$  should be first differentiated with respect to time and then takes the limit  $q_z \rightarrow 0$ . Eq. (10) is the formula for the energy flux in terms of normal mode coordinates from lattice dynamic point of view. It provides the basic starting point for studying the energy transmission across the interface.

### B. Energy Transmission

Once the energy flux formula Eq. (10) is obtained, we can further discuss the problem of energy transmission

across the interface. The idea for lattice dynamic approach to study energy transmission across the interface was first proposed in Ref. 8. Assuming an eigen mode lattice wave for Eq. (2) incident from one lead, it will be refracted by the interface. The reflected and transmitted waves are assumed the linear combination of the eigen mode lattice waves of Eq. (2) at each side of the lead. These amplitude transmissions are solved through the equations of motion for the boundary atoms. But it should be noted that these amplitude transmissions are not energy transmissions. What are their relation to the energy transmissions? As already cited in the introduction part of this paper, several assumptions<sup>8</sup> are made to calculate the energy transmissions from these amplitude transmissions. Apart from this problem, any eigenvector for Eq. (2) can be multiplied by a whatever coefficient and it is still the eigenvector. It means that the choice of eigenvector is not unique because of the linear nature of the harmonic system. This indeterminacy will complicate the calculation of the amplitude transmissions and makes the amplitude transmission coefficients non-unique. However the energy transmissions are determined by the system and have unique values. The key to this problem is energy conservation, which means that the energy flux from the left and right lead should be equal. In this part, we use the energy flux Eq. (10) derived from the energy continuity equation in the previous section to clarify these issues.

We assume that the vibration of the atoms for each incident/transmitted normal mode is

$$\tilde{u}_{l,i,n}^{\alpha}(\omega, \mathbf{q}) = \frac{1}{\sqrt{m_i}} \tilde{e}_{i,n}^{\alpha}(\mathbf{q}) e^{i(\mathbf{q} \cdot \mathbf{R}_i - \omega t)}, \quad (11)$$

where  $\tilde{e}_{i,n}^{\alpha}(\mathbf{q})$  is the eigenvector for dynamic matrix Eq. (2) and it satisfies  $\sum_{i,\alpha} \tilde{e}_{i,n}^{\alpha}(\mathbf{q}) \tilde{e}_{i,n'}^{*\alpha}(\mathbf{q}) = \delta_{n,n'}$ . It is obvious that our choice for the eigen mode is unique and deterministic. Compared with the choice of incident normal mode in Ref. 8, the difference is that the atomic mass should be included. The reason for this is simple: the eigenvectors of Eq. (2) are not the travelling wave solution for the system and its relation to travelling wave is to be divide by  $\sqrt{m_i}$  according to the definition of Eq. (2). We assume the same form, Eq. (11), for all the incident, reflected, and transmitted waves. When one particular mode  $\tilde{u}_{l,i,n}^{\alpha,L}(\omega, \mathbf{q})$  is incident from the left lead, it will be scattered by the interface. So the reflected wave is given as  $\sum_{n'} t_{n'n}^{L,L} \tilde{u}_{l,i,n'}^{\alpha,L}(\omega, -\mathbf{q}')$  and the transmitted wave is  $\sum_{n'} t_{n'n}^{R,L} \tilde{u}_{l,i,n'}^{\alpha,R}(\omega, \mathbf{q}'')$ . In these equations,  $t_{n'n}^{\sigma',\sigma}$  is the amplitude transmission/reflection coefficients from mode  $n$  in the lead  $\sigma = L$  to mode  $n'$  in lead  $\sigma' = R, L$ . Note that  $\mathbf{q}'$  and  $\mathbf{q}''$  satisfies  $\omega = \omega_{n'}(-\mathbf{q}') = \omega_{n'}(\mathbf{q}'')$ . Similar expression can be written down for the right lead. The total wave for one particular lead, say the left lead, is an arbitrary superposition of all these eigen modes. Thus,

the motion of the atoms is described by the wave:

$$\begin{aligned} \Psi_{l,i}^{\alpha,L}(\omega, t) &= \sum_n a_n^L \tilde{u}_{l,i,n}^{\alpha,L}(\omega, \mathbf{q}) \\ &+ \sum_n \left( \sum_{n',\sigma=L,R} a_{n'}^{\sigma} t_{n'n}^{\sigma,L} \right) \tilde{u}_{l,i,n}^{\alpha,L}(\omega, -\mathbf{q}'), \end{aligned} \quad (12)$$

where  $a_n^{\sigma}$  is an arbitrary amplitude of the mode  $n$  in lead  $\sigma$ . With the help of our newly derived energy flux Eq. (10) for lattice dynamics, after transforming Eq. (12) into normal mode coordinates, we can get the heat flux for the lead  $\sigma = L, R$ :

$$\bar{I}^{\sigma} = \frac{1}{V_{\sigma}} \sum_n \left( |a_n^{\sigma}|^2 - \left| \sum_{n',\sigma'} a_{n'}^{\sigma'} t_{nn'}^{\sigma\sigma'} \right|^2 \right) \omega_n^2 \frac{\partial \omega_n^{\sigma}(\mathbf{q})}{\partial q_z}. \quad (13)$$

Since the energy must be conserved, there is no net energy accumulation in the junction, which means that the time-averaged energy currents from both sides are equal,  $I^L \equiv I^R$ , where the energy currents  $I^{\sigma} = \bar{I}^{\sigma} \cdot S_{\sigma}$ ,  $\sigma = L, R$  and  $S_{\sigma}$  represents the cross area for each lead. This condition leads to the following identity for the transmission amplitudes,

$$\sum_{\sigma,n} t_{nn'}^{\sigma\sigma'} t_{nn''}^{*\sigma\sigma''} \tilde{v}_n^{\sigma} = \tilde{v}_{n'}^{\sigma'} \delta_{n'\sigma',n''\sigma''}, \quad \tilde{v}_n^{\sigma} = v_n^{\sigma} / l_z^{\sigma}, \quad (14)$$

where  $l_z^{\sigma}$  is the length of unit cell along the  $z$  direction,  $v_n^{\sigma} = \partial \omega_n^{\sigma} / \partial q_z$ . This equation is analogous to the unitarity condition for the scattering matrix in electronic transmission. To clearly understand the meaning of Eq. (14), we can write it into a matrix product equation  $\mathbf{t}^{\dagger} \tilde{\mathbf{v}} \mathbf{t} = \tilde{\mathbf{v}}$  with

$$\tilde{\mathbf{v}} = \begin{pmatrix} \tilde{v}_1^L & 0 & 0 & 0 & 0 & 0 \\ 0 & \tilde{v}_2^L & 0 & 0 & 0 & 0 \\ 0 & 0 & \dots & 0 & 0 & 0 \\ 0 & 0 & 0 & \tilde{v}_1^R & 0 & 0 \\ 0 & 0 & 0 & 0 & \tilde{v}_2^R & 0 \\ 0 & 0 & 0 & 0 & 0 & \dots \end{pmatrix}, \quad (15a)$$

$$\mathbf{t} = \begin{pmatrix} t_{11}^{LL} & t_{12}^{LL} & \dots & t_{11}^{LR} & \dots \\ t_{21}^{LL} & t_{22}^{LL} & \dots & t_{21}^{LR} & \dots \\ \dots & \dots & \dots & \dots & \dots \\ t_{11}^{RL} & t_{12}^{RL} & \dots & t_{11}^{RR} & \dots \\ t_{21}^{RL} & t_{22}^{RL} & \dots & t_{21}^{RR} & \dots \\ \dots & \dots & \dots & \dots & \dots \end{pmatrix}. \quad (15b)$$

The above expression and the technique we used are similar to the continuum case,<sup>12</sup> but the mathematics involved in the lattice dynamic framework is simpler and clearer. Several interesting conclusions can be made from Eq. (14) and Eq. (15).

(1) The amplitude transmissions from each lead are not independent. They must obey Eq. (14) so that the energy will be kept conserved. It means that which lead is chosen for calculating the energy transmission does not matter. They will give the same energy flux from either of the lead. In practice, this should be a good criterion

to check the validity of the algorithm in calculating the amplitude transmission.

(2) From the diagonal terms of Eq. (14), the energy transmission  $\tilde{T}_{n'n}^{\sigma'\sigma}$  from mode  $(\sigma, n)$ , which means  $\sigma$  lead and  $n$  branch, to the mode  $(\sigma', n')$  is given by

$$\tilde{T}_{n'n}^{\sigma'\sigma} = |t_{n'n}^{\sigma'\sigma}|^2 \frac{\tilde{v}_{n'}^{\sigma'}}{\tilde{v}_n^{\sigma}}. \quad (16)$$

The total reflected and transmitted energy transmission for  $(\sigma, n)$  is given by

$$\mathcal{R}_n^\sigma = \sum_{n'} |t_{n'n}^{\sigma\sigma}|^2 \frac{\tilde{v}_{n'}^\sigma}{\tilde{v}_n^\sigma}, \quad \mathcal{T}_n^\sigma = \sum_{n', \sigma' \neq \sigma} |t_{n'n}^{\sigma'\sigma}|^2 \frac{\tilde{v}_{n'}^{\sigma'}}{\tilde{v}_n^\sigma}, \quad (17a)$$

$$\mathcal{R}_n^\sigma + \mathcal{T}_n^\sigma \equiv 1. \quad (17b)$$

(3) The energy transmission's relation to atomic mass, lattice constant and the group velocity is explicitly expressed in Eq. (17a). It can be seen that the atom mass  $m_i$  for each lattice site  $\mathbf{R}_{l,i}$  should be considered in each eigen mode wave as in Eq. (11). Ref. 8 used  $t_{\mathbf{k}j} = \rho_A \sum_q v_{qz} A_q^2 / (\rho_B v_{0z} A_0^2)$  to calculate the energy transmission from the amplitude transmission  $A_q$ . This equation is correct only if the atomic masses are the same in a unit cell. In actuality, the ratio of Silicon mass density to Germanium mass density is about 0.4375 at temperature  $T = 300$  K, while the accurate coefficient should be  $28/72 \approx 0.389$  if the energy is conserved and lattice constants are same for both leads. Ref. 13 improved this by using the atomic mass ratio in the final energy transmission to keep energy conserved. But when the unit cell of system is composite, the choice of incident mode wave of Ref. 8 is wrong. It should be chosen as our Eq. (11). So the results of thermal conductance between metals and  $BaF_2$  in Ref. 8 are arguable using the method in Ref. 8. The lattice constant is also considered in Eq. (17a), which may have significant contribution when the difference in the lattice constants for the left and right lead crystal is large.

(4) Comparing with the continuum case<sup>11</sup>, we see an extra factor of the lattice dimension in  $z$  direction,  $l_z^2$ . This factor can be included in the amplitude transmission if we redefine our normal mode as that in Eq. (11) multiplied by  $\sqrt{V_{\text{cell}}}$ , where  $V_{\text{cell}}$  is the volume of a unit cell.

Next, we quantize Eq. (10) with

$$\hat{Q}_{\mathbf{q}}^n(t) = \sqrt{\frac{\hbar}{2\omega_n}} \left( \hat{a}_{n,\mathbf{q}} e^{-i\omega_n t} + \hat{a}_{n,-\mathbf{q}}^\dagger e^{i\omega_n t} \right), \quad (18a)$$

$$\dot{\hat{Q}}_{-\mathbf{q}}^n(t) = -i\sqrt{\frac{\hbar\omega_n}{2}} \left( \hat{a}_{n,-\mathbf{q}} e^{-i\omega_n t} - \hat{a}_{n,\mathbf{q}}^\dagger e^{i\omega_n t} \right). \quad (18b)$$

We get the quantization of the heat current  $\bar{I} = \frac{1}{V} \sum_{\mathbf{q},n} \hbar\omega_n(\mathbf{q})v_n(\mathbf{q})\hat{a}_{n,\mathbf{q}}^\dagger\hat{a}_{n,\mathbf{q}}$ . Similarly after quantizing Eq. (13) with the help of the relation Eq. (14), and taking

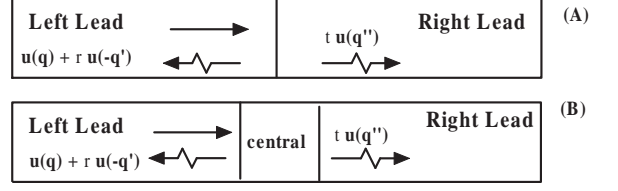


FIG. 1: Schematic show for scattering boundary condition.

thermal average, we can get the Kapitza conductance as

$$G_K = \lim_{\Delta T \rightarrow 0} \frac{\bar{I}}{\Delta T} = \frac{1}{V} \sum_{\mathbf{q},n,v_n>0} \hbar\omega_n(\mathbf{q})v_n(\mathbf{q})\mathcal{T}_n(\mathbf{q},\omega_n) \frac{\partial f(\omega_n,T)}{\partial T}, \quad (19)$$

where  $\mathcal{T}_n(\mathbf{q},\omega_n) = \sum_{n'} |t_{n'n}^{RL}|^2 \tilde{v}_{n'}^R / \tilde{v}_n^L$  and  $f(\omega_n, T)$  is the Bose-Einstein distribution at temperature  $T$ . The dispersion relation and group velocity refer to the left lead. In deriving Eq. (19), we have used the fact that phonons in the lead obey the Bose-Einstein distribution.

### C. Scattering Boundary Method

The central issue now is to have an efficient method to calculate the amplitude transmission coefficients across junctions at the atomistic level. Ref. 8 has proposed solving the amplitude transmissions through connecting boundary atoms for abrupt solid interface. But this appears to be a difficult problem for general complex interfaces. As illustrated in Fig. 1, the central part of atoms is not known so the method proposed in Ref. 8 will not work. Transfer matrix method can be used for simple 1D models with a few atoms in the central part to obtain analytical solutions. But this method is not numerically stable for a long 1D system (such as a disordered 1D system) or 3D systems because the errors get amplified by continuous multiplications of a matrix with eigenvalues larger than 1. In fact, we have tried transfer matrix method for the nanotube junction and found large numerical errors of 30% or more.

Here we propose what we call the scattering boundary equation method (SBM) as a solution. Each atom in the system satisfies the dynamic equation,  $-m_i\omega^2\mathbf{u}_i + \sum_j K_{ij}(\mathbf{u}_i - \mathbf{u}_j) = 0$ , where the  $3 \times 3$  matrix  $K_{ij}$  is the force constants between atom  $i$  and  $j$ . The boundary conditions are of the form  $\tilde{\mathbf{u}}_{q,n'} + \sum_n r_n \tilde{\mathbf{u}}_{-q,n}$  for the incoming and reflected waves and  $\sum_n t_n \tilde{\mathbf{u}}'_{q',n}$  for the outgoing waves, where  $\tilde{\mathbf{u}}_{q,n}$  and  $\tilde{\mathbf{u}}'_{q',n}$  are the eigen modes on the left and right leads, while the reflection and transmission coefficients  $r_n$  and  $t_n$  are unknown. These equations

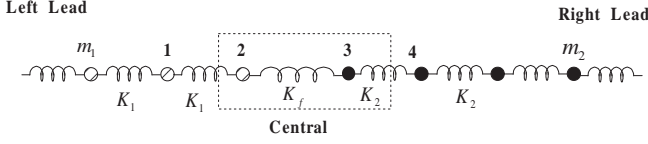


FIG. 2: Schematic show for 1D acoustically mismatched chain model.

in matrix form are illustrated as

$$\begin{pmatrix} \cdots \\ \vdots & K_{ii} & -K_{ij} \\ 1 & & & -\tilde{u}_{-q,n} & -\tilde{u}'_{q',n} \end{pmatrix} \begin{pmatrix} u_1 \\ \vdots \\ u_m \\ r_n \\ t_n \end{pmatrix} = \begin{pmatrix} 0 \\ \vdots \\ 0 \\ \tilde{u}_{q,n} \\ 0 \end{pmatrix}, \quad (20)$$

where  $K_{ii} = -m_i\omega^2 + \sum_j K_{ij}$ . These equations can be both analytically and numerically solved by the conventional method if the matrix is square. In some cases for higher dimensions, however, the boundary conditions are complicated and the number of equations may be larger than that of variables. But these equations are not linearly independent. Nevertheless, these equations are consistent and simultaneous. Under this condition the scattering boundary equations can still be solved numerically by the standard singular value decomposition method<sup>14</sup>.

#### D. Analytic Results on 1D Model

To demonstrate the formulas obtained in the previous part and the scattering boundary equation method, we give some analytic results on a toy 1D model. More realistic material solid junctions, e.g. nanotube conjunction and Si-Ge interface, will be discussed in the next section. We consider two acoustically mismatched chains of different atomic masses  $m_1, m_2$ , connected with springs of different stiffness  $K_1, K_2$ , and lattice constant  $a, b$ , on each side as illustrated in Fig. 2. In the central part they are connected by a spring with stiffness  $K_f$ . The dynamic matrix for the 1D chain gives the eigenvector  $\tilde{e}_l = e^{iq_1 x_l}$  and  $\omega_L^2 = \frac{2K}{m}(1 - \cos(qa))$ . From Eq. (11), the incident, reflected and transmitted waves from the left lead can be written as

$$u_{Lr} = \left( \frac{1}{\sqrt{m_1}} e^{iq_1 x} + t^{LL} \frac{1}{\sqrt{m_1}} e^{-iq_1 x} \right) e^{-i\omega t}, \quad (21a)$$

$$u_{Lt} = t^{RL} \frac{1}{\sqrt{m_2}} e^{iq_2 x} e^{-i\omega t}, \quad (21b)$$

where, following the notation of Eq. (12),  $t^{LL}$  and  $t^{RL}$  are the reflected and transmitted amplitudes. Similar expressions can be written down for the wave incident

from the right lead as

$$u_{Rr} = \left( \frac{1}{\sqrt{m_2}} e^{-iq_2 x} + t^{RR} \frac{1}{\sqrt{m_2}} e^{iq_2 x} \right) e^{-i\omega t}, \quad (22a)$$

$$u_{Rt} = t^{LR} \frac{1}{\sqrt{m_1}} e^{-iq_1 x} e^{-i\omega t}. \quad (22b)$$

As illustrated in the schematic Fig. 2, there are two atoms, labelled 2 and 3 in the figure, in the connecting part. The equations of motion for the two atoms are

$$(-m_1\omega^2 + K_1 + K_f)u_2 - K_1u_1 - K_fu_3 = 0, \quad (23a)$$

$$(-m_2\omega^2 + K_f + K_2)u_3 - K_fu_2 - K_2u_4 = 0. \quad (23b)$$

For wave incident from the left lead, the SBM equations can be expressed as

$$\begin{pmatrix} -K_1 & K_{22} & -K_f & 0 & 0 & 0 \\ 0 & -K_f & K_{33} & -K_2 & 0 & 0 \\ 1 & 0 & 0 & 0 & \frac{-e^{-iq_1 x_1}}{\sqrt{m_1}} & 0 \\ 0 & 1 & 0 & 0 & \frac{-e^{-iq_1 x_2}}{\sqrt{m_1}} & 0 \\ 0 & 0 & 1 & 0 & 0 & \frac{-e^{iq_2 x_3}}{\sqrt{m_2}} \\ 0 & 0 & 0 & 1 & 0 & \frac{-e^{iq_2 x_4}}{\sqrt{m_2}} \end{pmatrix} \begin{pmatrix} u_1 \\ u_2 \\ u_3 \\ u_4 \\ t^{LL} \\ t^{RL} \end{pmatrix} = \begin{pmatrix} 0 \\ 0 \\ \frac{e^{iq_1 x_1}}{\sqrt{m_1}} \\ \frac{e^{iq_1 x_2}}{\sqrt{m_1}} \\ 0 \\ 0 \end{pmatrix}, \quad (24)$$

where  $K_{22} = -m_1\omega^2 + K_1 + K_f$ ,  $K_{33} = -m_2\omega^2 + K_f + K_2$  and  $q_1, q_2$  satisfy that  $\omega_L(q_1) = \omega_R(q_2)$ . For simplicity, we only consider the condition that the two spring chains are connected directly by the spring  $K_f$ . If there are more atoms at the central part, we only need to add equations like Eq. (23) for these atoms to Eq. (24). But the scattering boundary condition in Eq. (24), last four rows, does not change. From Eq. (24), we can get

$$\begin{aligned} t^{LL} &= [-K_f e^{iq_1 x_2} + (\frac{K_{33}}{K_f} - \frac{K_2}{K_f} e^{iq_2 b}) \\ &\quad (K_{22} e^{iq_1 x_2} - K_1 e^{iq_1 x_1})] / [(\frac{K_{33}}{K_f} - \frac{K_2}{K_f} e^{iq_2 b}) \\ &\quad (K_{22} e^{-iq_1 x_2} - K_1 e^{-iq_1 x_1}) + K_f e^{-iq_1 x_2}], \end{aligned} \quad (25a)$$

$$\begin{aligned} t^{RL} &= \sqrt{\frac{m_2}{m_1}} [(K_{22} e^{iq_1 x_2} - K_1 e^{iq_1 x_1}) \\ &\quad + (K_{22} e^{iq_1 x_2} - K_1 e^{iq_1 x_1})] / K_f. \end{aligned} \quad (25b)$$

Similarly for wave incident from the right lead, we have SBM equations

$$\begin{pmatrix} -K_1 & K_{22} & -K_f & 0 & 0 & 0 \\ 0 & -K_f & K_{33} & -K_2 & 0 & 0 \\ 1 & 0 & 0 & 0 & 0 & \frac{-e^{-iq_1 x_1}}{\sqrt{m_1}} \\ 0 & 1 & 0 & 0 & 0 & \frac{-e^{-iq_1 x_2}}{\sqrt{m_1}} \\ 0 & 0 & 1 & 0 & \frac{-e^{iq_2 x_3}}{\sqrt{m_2}} & 0 \\ 0 & 0 & 0 & 1 & \frac{-e^{iq_2 x_4}}{\sqrt{m_2}} & 0 \end{pmatrix} \begin{pmatrix} u_1 \\ u_2 \\ u_3 \\ u_4 \\ t^{RR} \\ t^{LR} \end{pmatrix} = \begin{pmatrix} 0 \\ 0 \\ 0 \\ 0 \\ \frac{e^{-iq_2 x_3}}{\sqrt{m_2}} \\ \frac{e^{-iq_2 x_4}}{\sqrt{m_2}} \end{pmatrix}. \quad (26)$$

From Eq. (26), we can also get  $t^{RR}$  and  $t^{LR}$ . Next we construct Eq. (15) for 1D model as

$$\mathbf{t} = \begin{pmatrix} t^{LL} & t^{LR} \\ t^{RL} & t^{RR} \end{pmatrix}, \quad \mathbf{v} = \begin{pmatrix} \frac{v^L}{a} & 0 \\ 0 & \frac{v^R}{b} \end{pmatrix}. \quad (27)$$

Matrix Eq. (15),  $\mathbf{t}^\dagger \tilde{\mathbf{v}} \mathbf{t} = \tilde{\mathbf{v}}$ , gives four equations for this 1D model,

$$|t^{LL}|^2 \frac{v^L}{a} + |t^{RL}|^2 \frac{v^R}{b} = \frac{v^L}{a}, \quad (28a)$$

$$|t^{RR}|^2 \frac{v^R}{b} + |t^{LR}|^2 \frac{v^L}{a} = \frac{v^R}{b}, \quad (28b)$$

$$t^{LL*} t^{LR} \frac{v^L}{a} + t^{RL*} t^{RR} \frac{v^R}{b} = 0, \quad (28c)$$

$$t^{LL} t^{LR*} \frac{v^L}{a} + t^{RL} t^{RR*} \frac{v^R}{b} = 0. \quad (28d)$$

These equations can be easily verified using the results from Eqs. (24, 25, 26). These four equations also guarantee the same energy transmission both for the left and the right lead, that is

$$\mathcal{T}^L = \mathcal{T}^R = |t^{RL}|^2 \frac{v^R}{b} = |t^{LR}|^2 \frac{v^L}{a}. \quad (29)$$

It can be easily seen from the simple 1D case that amplitude transmissions from the left and right lead are not independent and should satisfy the relation (14) to keep the energy conserved.

Furthermore, for 1D quantum thermal energy current, with the help of the relation (14), after quantizing Eq. (13), we get the formula

$$\bar{I} = \frac{1}{2\pi} \sum_n \int_{\omega_{\min}}^{\omega_{\max}} d\omega \hbar \omega \left( f(\omega, T_L) - f(\omega, T_R) \right) T_n(\omega), \quad (30)$$

where  $T_n(\omega) = \sum_m |t_{mn}^{RL}|^2 \tilde{v}_n^R / \tilde{v}_m^L$  is the energy transmission probability,  $f(\omega, T_\sigma)$  is the Bose-Einstein distribution for the left or right lead. Eq. (30) is the Landauer formula for quantum thermal energy flow in one dimension.

### III. SIMULATION

In this section, we report our results for two kinds of solid junctions: nanotube junction and the Si-Ge interface. Nanotube has been found to be good candidate for thermal conduction materials and the thermal conduction has been improved through adding nanotube mixture<sup>15</sup>. But the interface between nanotubes are inevitable. How they will affect thermal conduction becomes an interesting problem. Thermal conduction across the Si-Ge interface has been studied by Ref. 8 using the simplified *fcc* lattice model and recently by

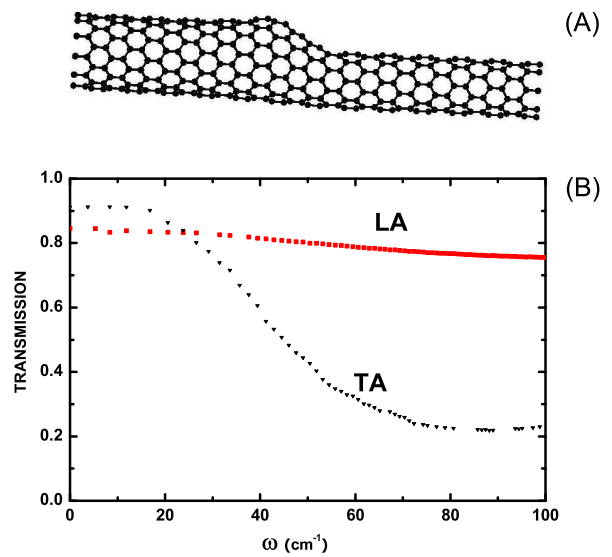


FIG. 3: (a) Structure of a (11,0) and (8,0) nanotube junction. (b) The energy transition  $T_n(\omega)$  as a function of angular frequency  $\omega$ .

Ref. 13 in diamond structure with equal lattice constants for Si and Ge and with *fcc* neighboring atoms considered. In our paper, we will consider more realistic crystal structure for Si and Ge to investigate the energy transmission dependence on incident angle and low-temperature scaling behavior of Kapitza conductance.

#### A. Nanotube Junction

The semiconductor nanotube junction structure (11,0) and (8,0) is first constructed by a geometrical method as in Ref. 16. However there are many defects in the geometrically constructed structure. Next we optimize the junction structure by a second-generation Brenner potential<sup>17</sup> to let the atoms get their equilibrium positions. The optimized structure is shown in Fig. 3(a). Then under small displacement, the force constants are derived numerically from the same potential. The phonon dispersion calculated from these linearized force constants for nanotube (11,0) is illustrated in Fig. 4, in which four acoustic branches are considered for energy transport: the longitudinal mode (LA), doubly degenerate transverse mode (TA), and the unique twist mode (TW) in nanotubes.

Following the SBM method, the SBM equations are constructed and it involves 504 equations and 455 variables. However, some equations are not linearly independent and are consistent because the motion for each atom is connected with the motions of others forming traveling waves and they are confined together to construct the nanotube structure. We also numerically verified the consistency of these equations through the calculation of ranks for SBM equations. The rank we get is equal to 455 within numerical accuracy, which is equal to the number of variables. These equations are solved through

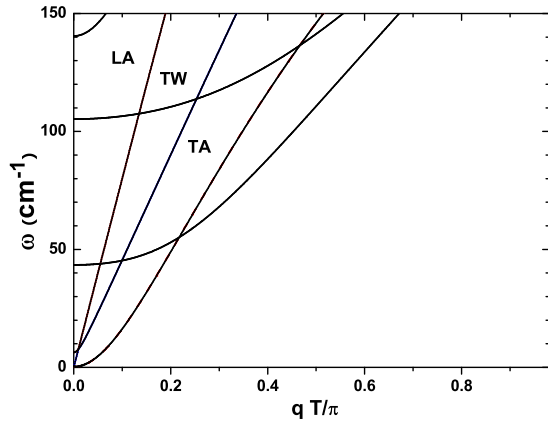


FIG. 4: Phonon dispersion for nanotube (11,0). The wave number  $q$  is expressed in terms of the length of nanotube translation vector  $T$ .

the standard singular value decomposition method<sup>14</sup>.

We then discuss the SBM results of the transmission coefficients for a nanotube junction, shown in Fig. 3(b). Although all modes of a given frequency are considered, we did not find mode-mixing or mode-conversion behavior among acoustic modes at the lower frequency range. For example, the reflected and the transmitted waves across the junction for the incident LA mode waves are both only LA modes. We think that this is due to the high symmetrical properties of atomic motion for nanotubes. Each travelling wave on nanotube has its own symmetrical property resulting from the symmetry of the nanotube structure. The symmetry on the left and right lead is different. It is hard to convert one specific high symmetrical motion to the other different symmetrical motion through the conjunction except when the symmetrical properties on each lead are the same. We think that this kind of mismatch in the symmetry of motion for nanotubes will play an important role in the thermal conduction of nanotube mixtures.

The LA modes are common symmetrical motion for both the left and right lead. The transmission for LA mode stays around 0.8 with only small changes. This value is below the AM model prediction<sup>18</sup> of 0.98 with the longitudinal group velocity  $20.18 \text{ kms}^{-1}$  and  $20.95 \text{ kms}^{-1}$  for (11,0) and (8,0). In contrast, the transmissions of the TW mode and many other optical modes are nearly zero or very small. This appears related to the difference in rotational symmetries of these modes. The transmission for TA mode decreases with frequency. This can be accounted for two reasons: (1) Although the TA mode is a common symmetry for both left and right lead, the kind of transverse symmetry is destroyed by the central junction part. It can be seen from Fig. 3 that the central junction part does not have transverse symmetry. (2) There is a mismatch of dispersion relation for TA mode because the TA mode has a nearly quadratic dispersion

relation, as illustrated in Fig. 4. These reasons will affect the transmission for TA mode at high frequency when the vibration motion of atoms is fast.

So it can be seen from above that energy transmission across nanotube junctions is strongly dependent on symmetry property of the lead nanotube. This symmetry dependence is also observed by molecular dynamics.<sup>19</sup> Usually such mismatch in symmetry will reduce the number of possible transmission modes and thus blocks the thermal conduction across the junction. We also propose that this kind of mode-dependent transmission behavior may be important for further application such as phonon filters.

## B. Si-Ge Interface

The Kapitza conductance across the Si-Ge interface have been calculated by lattice dynamic method in Ref. 8 using the simplified *fcc* lattice model and recently by Ref. 13 in diamond structure with *fcc* neighboring atoms considered. However, the relation of energy transmission to the incident wave angle and the temperature dependence of Kapitza conductance at lower temperature remains unclear. Here we use our newly derived formulas combined with the simulation to get an understanding of these problems in more realistic Si-Ge structure. We first discuss the energy transmission's relation to the incident angles and to wave mode conversion at the interface. The Kapitza conductance across Si and Ge interface is also calculated and its scaling law in relation to temperature at low-temperature regime is numerically analyzed.

The lattice structure for Si and Ge crystal we considered is the diamond structure. The atomic mass for Si and Ge are  $28 \text{ amu}$  and  $72.61 \text{ amu}$ . The lattice constants for each conventional unit cell are  $a = 5.43 \text{ \AA}$  and  $a = 5.658 \text{ \AA}$ , respectively. We use the Tersoff potential<sup>17</sup> under small displacement to get the linearized force con-

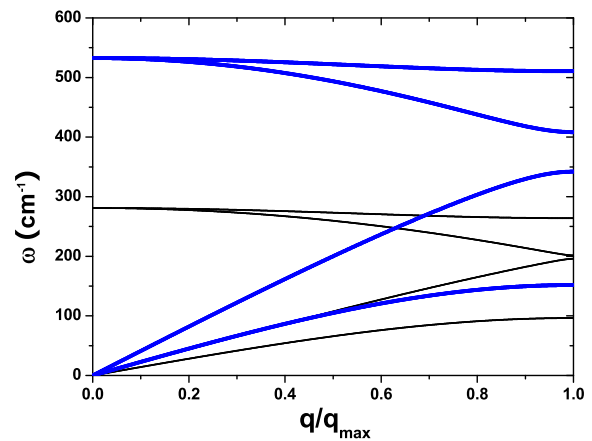


FIG. 5: Phonon dispersion along  $\Gamma - L$  for Si and Ge. The thick lines are for Si and the thin lines for Ge. The wave number is in terms of the maximum value along  $\Gamma - L$  direction.



stants. By Tersoff potential truncation function,<sup>17</sup> only the nearest 4 atoms are considered for each atom with the distance  $\sqrt{3}a/4$ . We choose the primary cell consisting of two atoms  $(0, 0, 0)$  and  $(a/4, a/4, a/4)$  to construct the dynamic matrix. The phonon dispersion for Si and Ge along the  $\Gamma - L$  direction can be calculated through the linearized force constants from the dynamic matrix and are illustrated in Fig. 5. The maximum LA branch along  $\Gamma - L$  frequency for Si and Ge are  $343 \text{ cm}^{-1}$  and  $196 \text{ cm}^{-1}$ . It can be seen that the linearized force constants for the nearest atoms well reproduce the Si and Ge phonon dispersion.<sup>20</sup> The group velocity is calculated through

$$v_g = \frac{1}{2\omega} \frac{\tilde{\mathbf{e}}^\dagger \frac{\partial \mathbf{D}}{\partial \mathbf{q}} \tilde{\mathbf{e}}}{\tilde{\mathbf{e}}^\dagger \cdot \tilde{\mathbf{e}}}, \quad (31)$$

where  $\mathbf{D}$  is the dynamic matrix and  $\tilde{\mathbf{e}}$  the eigenvector as shown in Eq. (2). The group velocity of LA branch phonons along the  $\Gamma - L$  direction for Si and Ge is about  $7.8 \text{ Km/s}$  and  $4.4 \text{ Km/s}$ .

For the Si or Ge diamond structure, there are six modes of vibration as illustrated in Fig. 5, among which three branches are acoustic and other three ones are optical. Using Eq. (11) when one mode of wave  $\tilde{u}_{l,i,n}^\alpha(\omega, \mathbf{q}) = \frac{1}{\sqrt{m_{\text{Si}}}} \tilde{e}_{i,n}^\alpha(\mathbf{q}) e^{i(\mathbf{q} \cdot \mathbf{R}_i - \omega t)}$  is incident from the lead, it has three modes of reflected wave and three modes of transmitted wave. Due to linearity of the system, the frequency does not change during refraction. We choose the Si-Ge interface with normal in  $[001]$  direction. Since the system is homogeneous in the  $x$  and  $y$  direction, the reflected waves and the transmitted waves have the same momentum in these directions  $q'_x, q''_x = q_x$ ;  $q'_y, q''_y = q_y$ .  $q'_z$  and  $q''_z$  is found to satisfy  $\omega(\mathbf{q}) = \omega_{\text{Si}}(\mathbf{q}') = \omega_{\text{Ge}}(\mathbf{q}'')$ . If  $q'_z$  or  $q''_z$  is complex,  $\text{Im}[q'_z]$  or  $\text{Im}[q''_z]$  should be negative. The force constants for the Si-Ge interface are chosen as  $K_{ij} = (K_{ij}^{\text{Si}} + K_{ij}^{\text{Ge}})/2$ . Each atom in the incident lead part has the motion  $\mathbf{u}_{\text{reflect}} = \tilde{\mathbf{u}}(\mathbf{q}) + r_1 \tilde{\mathbf{u}}(-\mathbf{q}'_1) + r_2 \tilde{\mathbf{u}}(-\mathbf{q}'_2) + r_3 \tilde{\mathbf{u}}(-\mathbf{q}'_3)$ ; similarly for the motion in the transmitted wave  $\mathbf{u}_{\text{transmit}} = t_1 \tilde{\mathbf{u}}(\mathbf{q}''_1) + t_2 \tilde{\mathbf{u}}(\mathbf{q}''_2) + t_3 \tilde{\mathbf{u}}(\mathbf{q}''_3)$ . Connecting the Si-Ge interface provides us two equations of motion,

$$(-m_{\text{Si}}\omega^2 + \sum_j \mathbf{K}_{ij}) \mathbf{u}_i - \sum_j \mathbf{K}_{ij} \mathbf{u}_j = 0, \quad (32)$$

$$(-m_{\text{Ge}}\omega^2 + \sum_j \mathbf{K}_{ij}) \mathbf{u}_i - \sum_j \mathbf{K}_{ij} \mathbf{u}_j = 0. \quad (33)$$

There are all 8 different atoms in the above two equations. Each atom should have the form of solution of the reflected  $\mathbf{u}_{\text{reflect}}$  or the transmitted  $\mathbf{u}_{\text{transmit}}$ , which depends on its position. The scattering boundary equations are constructed. There are 30 equations (two equations of motion give 6 and another 8 atoms taking the scattering boundary condition solution give 24) and 30 variables (8 atoms give 24 and 6 for reflected coefficients  $\mathbf{r}$  and transmitted coefficients  $\mathbf{t}$ ) in the scattering boundary equations. This set of equations can be solved by a

conventional method. When  $\mathbf{r}$  and  $\mathbf{t}$  is obtained, the energy reflection coefficients  $R$  and transmission coefficients  $T$  for each mode are given by summation of Eq. (16).

We first report the result of the dependence of energy transmission on the incident angle. A continuum wave incident on the surface whose wave vector makes an angle  $\theta$  with the surface normal is refracted in accordance with Snell's law. Does the refraction of phonon incident on the solid interface observe the Snell's law? Is there any new character for phonon refraction? We calculated the energy transmission for LA mode incident from Si to Ge and incident from Ge to Si. The results are illustrated in Fig. 6 and Fig. 7.

It can be seen from Fig. 6 that when the angle  $\theta$  for the phonon incident from Si to Ge increases, energy transmission decreases slowly. But once the angle is larger than  $80^\circ$ , the transmission decreases rapidly. In contrast to the transmission from Si to Ge, LA mode wave transmission from Ge to Si shows a rich character as illustrated in Fig. 7. For wave with the incident angle  $\theta \neq 0$ , the transmission first decreases with the increase of frequency. But when the frequency goes over a certain value, for example  $\omega = 93 \text{ cm}^{-1}$  for  $\theta = 36^\circ$ , the transmission begins to increase. This behavior can be understood by the mode conversion at the interface. It

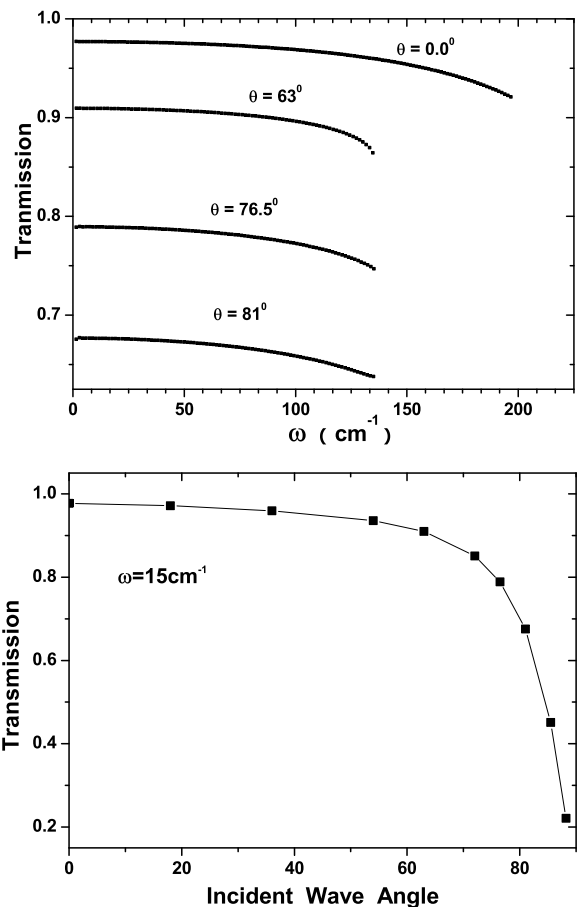


FIG. 6: Dependence of energy transmission on the incident angle. LA phonon incident from Si to Ge.



can be seen from Fig. 5 that the maximum frequency for  $TA$  modes in Ge is about  $98 \text{ cm}^{-1}$ . When the frequency is below this value, there are  $TA$  modes for the reflected wave; but over this value, the reflected wave can not be converted into  $TA$  modes. So due to lack of reflected modes, the transmission increases.

Furthermore, for  $LA$  waves incident from Ge to Si, there exists a critical value, about  $42^\circ$ , above which transmission equals 0. We can estimate the critical angle with the help of Snell's law for continuum wave. The group velocities for normal incident waves in direction  $[001]$  are  $v_g^{Si} \approx 6.87 \text{ Km/s}$  and  $v_g^{Ge} \approx 3.78 \text{ Km/s}$ . The Snell's law gives the critical angle from Ge to Si  $\theta_c = \sin^{-1}(v_g^{Ge}/v_g^{Si}) = 33.4^\circ$ . This value is a little lower than the observed critical angle value. Nevertheless, we think that the Snell's law gives a rough estimation of the critical value for the critical incident angle for phonons.

When the incident waves from Si to Ge and from Ge to Si are both normal to the surface ( $\theta = 0$ ), the energy transmission from both sides are about the same 0.98. We use the acoustic mismatch model<sup>18</sup> to estimate  $4Z_{Si}Z_{Ge}/(Z_{Si} + Z_{Ge})^2 \approx 0.97$ . It can be seen that the acoustic mismatch model describes the transmission for normal incident waves well.

The Kapitza conductance with change of temperature

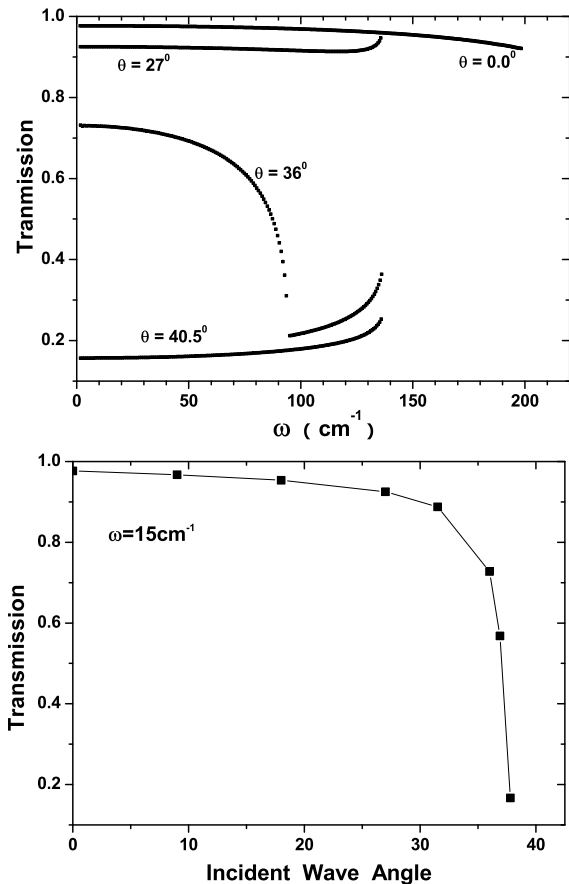


FIG. 7: Dependence of energy transmission on the incident angle.  $LA$  phonon incident from Ge to Si.

is calculated using Eq. (19). The results for Kapitza conductance and heat capacity using our linearized force constants are illustrated in Fig. 8. The Kapitza conductance for Si-Ge  $[100]$  interface calculated from our model is  $G_K = 4.6 \times 10^8 \text{ WK}^{-1} \text{ m}^{-2}$  when  $T = 200 \text{ K}$ . When the temperature goes over  $200 \text{ K}$ , we find that the Kapitza conductance changes little with the temperature and is saturated. For comparison, we plotted the heat capacity in Fig. 8. It can be seen from the figure that the heat capacity continues to increase with the temperature when  $T > 200 \text{ K}$ . In comparison with the heat capacity, the saturation of Kapitza conductance can be accounted by little contribution of energy transmission from high frequencies. At low temperatures, as illustrated in inset of Fig. 8, the Kapitza conductance scales as  $T^{2.87}$ , while the heat capacity scales as  $T^3$  in accordance with the Debye model. We have sampled enough points in the first Brillouin zone to ensure that Kapitza conductance and heat capacity converge numerically. However, due to the small deviation from 3, we cannot rule out the possibility that the exponent for Kapitza conduction is also 3. Ref. 8 reported that Kapitza conductance scales as  $T^3$  at low temperatures for  $fcc$  interface irrespective of the properties for the left and right lead. The Kapitza conductance's dependence on temperature is an intriguing problem<sup>5</sup>, with much experimental work done in this

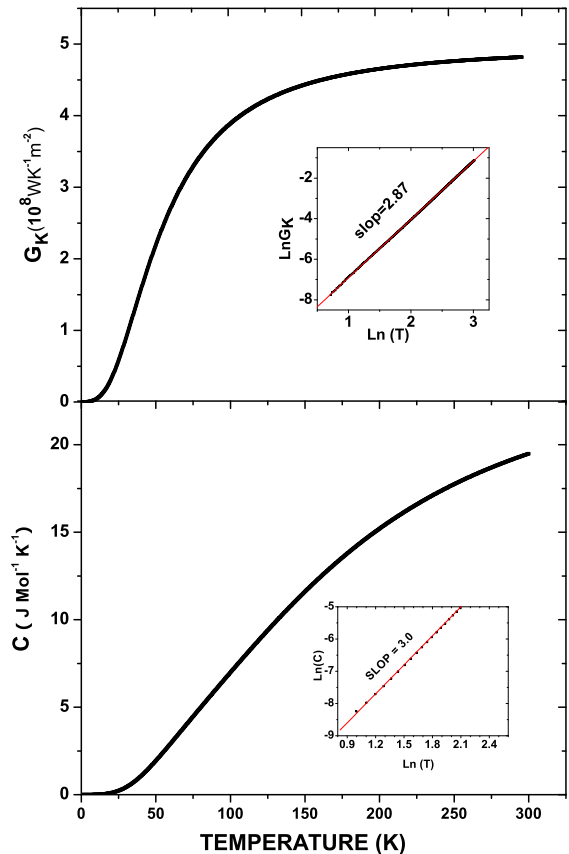


FIG. 8: Kapitza conductance and specific heat from linearized Tersoff potential.

field. Most experiments gave  $T^\alpha$  with  $\alpha \leq 3$  for solid interface as reviewed in Ref. 5. So far no experimental result is available for the temperature dependence of the Si-Ge interface. What value should it be is an interesting problem. Compared with the results of Ref. 8, our discrepancy from  $T^3$  comes from the anisotropy of the energy transmission because of the diamond structure is used for the calculation of the transmission, while Ref. 8 took the isotropic assumption in their calculation.

#### IV. CONCLUSION

In summary, we derive expressions for energy flux in terms of lattice normal mode coordinates. Energy transmission across solid junctions from lattice dynamic point of view is given and its relation with atom masses, lattice constants, and group velocities is also clarified. A scattering boundary method (SBM) is proposed for calculating the amplitude transmission across solid junction. Our calculation shows a mode-dependent transmission in nanotube junction due to the high symmetry vibrating motion for nanotube atoms, indicating its possible important role in nanotube mixture thermal conductance. Energy transmission and Kapitza conductance across the Si-Ge interface are calculated for the Si-Ge diamond-type structure from linearized Tersoff potential. It is shown that the energy transmission across the Si-Ge interface depends on the incident angle and on the interface mode conversion. A critical incident angle about

$42^\circ$  is numerically found for waves incident from Ge to Si. The critical angle in the reverse direction is much larger. The Kapitza conductance saturates to about  $G_K = 4.6 \times 10^8 \text{WK}^{-1}\text{m}^{-2}$  for  $T > 200 \text{K}$ . We numerically get its scaling law  $T^{2.87}$  for [001] interface at low temperature.

In additions, we remark that

(1) Eq. (14) and Eq. (15) are the basic relations for amplitude transmissions in linear systems, irrespective of the details of junction part. The results for any algorithm to calculate amplitude transmission from lattice point of view should satisfy these relations to keep the energy conserved. It dose not matter which lead to be chosen for the energy transmission because the energy flux will be the same according to Eq. (14). So Eq. (14) provides a criterion for checking the validity of the algorithm.

(2) Lattice dynamic approach to solid junction is only under linear approximation, which may be accurate at low temperatures. However, for high temperature the nonlinear effect or anharmonic effect has to be considered. How to include the effect of nonlinearity into phonon scattering at the solid junction will be an interesting problem.

#### V. ACKNOWLEDGEMENTS

This work is supported in part by a Faculty Research Grant of National University of Singapore. We thank Lin Yi and Nan Zeng for discussions.

- 
- <sup>1</sup> A. Balandin and K. L. Wang, Phys. Rev. B **58**, 1544 (1998); B. Li, L. Wang, and G. Casati, Phys. Rev. Lett. **93**, 184301 (2004).  
<sup>2</sup> S. Lepri, R. Livi, and A. Politi, Phys. Rep. **377**, 1 (2003). J.-S. Wang and B. Li, Phys. Rev. Lett. **92**, 074302 (2004).  
<sup>3</sup> K. Schwab *et al.*, Nature **404**, 974 (2000).  
<sup>4</sup> D. G. Cahill *et al.*, J. Appl. Phys. **93**, 793 (2003).  
<sup>5</sup> E. T. Swartz and R. O. Pohl, Rev. Mod. Phys. **61**, 605 (1989); P. L. Kapitza, J. Phys. (Moscow) **4**, 181 (1941).  
<sup>6</sup> C. L. Tien and G. Chen, J. Heat Transfer, **116**, 799 (1994); G. Chen, Phys. Rev. B **57**, 14958 (1998).  
<sup>7</sup> B.C. Daly *et al.*, Phys. Rev. B **66**, 024301 (2002); P. K. Schelling, S. R. Phillpot and P. Keblinski, Appl. Phys. Lett. **80**, 2848 (2002).  
<sup>8</sup> D. A. Young and H. J. Maris, Phys. Rev. B **40**, 3685 (1989); R. J. Stoner and H. J. Maris, Phys. Rev. B **48**, 16373 (1993).  
<sup>9</sup> N. Mingo and Y. Liu, Phys. Rev. B **68**, 245406 (2003).  
<sup>10</sup> R. Landauer, IBM J. Res. Dev. **1**, 223 (1957).  
<sup>11</sup> L. G. C. Rego and G. Kirczenow, Phys. Rev. Lett. **81**, 232 (1998); M. P. Blencowe, Phys. Rev. B **59**, 4992 (1999).  
<sup>12</sup> P. Yang, Ph. D. thesis, *Thermal Transport in Mesoscopic Dielectric Systems*, McGill University, 2004, unpublished.  
<sup>13</sup> H. Zhao and J. B. Freund, J. Appl. Phys **97**, 024903 (2005); *ibid*, **97**, 109901 (2005).  
<sup>14</sup> W. H. Press, *et al.*, *Numerical Recipes in C*, 2nd Ed., Cambridge University Press, 2002, p.59.  
<sup>15</sup> S. U. S. Choi *et al.*, Appl. Phys. Lett. **79**, 2252 (2001); M. J. Biercuk *et al.*, Appl. Phys. Lett. **80**, 2767 (2002).  
<sup>16</sup> R. Saito, G. Dresselhaus, and M. S. Dresselhaus, *Physical Properties of Carbons Nanotubes*, Imperial College Press, 1998, p115.  
<sup>17</sup> D. W. Brenner *et al.*, J. Phys.: Condens. Matter. **14**, 783 (2002); J. Tersoff, Phys. Rev. B **39**, (5566) 1989.  
<sup>18</sup> W. A. Little, Can. J. Phys. **37**, 334 (1959).  
<sup>19</sup> S. Shenogin *et al.*, J. Appl. Phys. **95**, 8136 (2004);  
<sup>20</sup> R. Tubino, L. Piseri, and G. Zerbi, the J. Chem. Phys. **56**, 1022 (1972); Giannozzi *et al.*, Phy. Rev. B **43**, 7231 (1991).